Journal of Engineering Physics and Thermophysics, Vol. 81, No. 1, 2008

DYNAMICS OF THE VISCOUS INTERACTION OF A RING VORTEX WITH A FLAT SCREEN

N. A. Vladimirova

UDC 532.526.2, 532.626.4, 532.526.5, 519.6

A separation turbulent flow has been mathematically simulated on the basis of numerical solution of nonstationary Navier–Stokes equations for determining the dynamics of viscous interaction of a ring vortex with a flat screen. The problem was solved for an axisymmetric turbulent flow at Reynolds numbers falling within the range 10^5–10^7. On the basis of the calculation data obtained, the interaction of a ring vortex with a turbulent flow induced on the screen and with the secondary ring vortices was investigated. The data obtained are in qualitative agreement with the analogous data obtained by other authors with the use of the discrete-vortex method and the boundary-layer theory as well as with the available experimental and calculation data obtained for a laminar flow.

Introduction. The most complete computational-theoretical investigations of the problem on the interaction of a ring vortex with a flat screen under turbulent-flow conditions at large Reynolds numbers were carried out in [1]. The authors of this work used the discrete-vortex method and the turbulent-boundary layer theory in their investigations. The nonstationary problem on the movement of a primary ring vortex to a screen and its interaction with the secondary vortices was solved in the nonviscous formulation with the use of the discrete-vortex method, and the parameters of the secondary ring vortices generated in the process of separation of the turbulent boundary layer induced on the screen were determined using the integral momentum relation of the theory of a turbulent axisymmetric radial boundary layer. In [2–9], the self-induced movement of a vortex ring to a flat screen was theoretically and experimentally investigated for an ideal viscous fluid flow at small Reynolds numbers. To this point the interaction of a ring vortex with a flat screen under the turbulent-flow conditions, to which large Reynolds numbers falling within the range 10^5–10^7 correspond, has not been investigated experimentally and theoretically on the basis of numerical solution of Navier–Stokes equations.

Formulation of the Problem. The problem on the viscous interaction of a ring solid vortex with a flat solid screen is solved numerally. A separation turbulent flow, giving an idea of the dynamics of the viscous interaction of a ring vortex with a turbulent near-wall flow generated on a flat solid screen, is mathematically simulated on the basis of solution of nonstationary Reynolds-averaged Navier–Stokes (RANS) equations with the use of the program complex ANSYS/CFX, ANSYS Inc. The equations of viscous-gas motion are numerically integrated using the finite-volume method, a numerical scheme of high order with respect to time and space for convective and viscous terms, and an improved two-parameter k–ω model of turbulence (Shear-Stress-Transport model) [10] that allows one to determine the characteristics of turbulent near-wall viscous flows with separation and without separation with a high degree of accuracy and to simulate a turbulent recirculation flow in the separation zones.

The problem was solved in the following formulation. At the initial instant of time t_0, a ring solid vortex of radius R_0 with a circulation Γ_0 and a circular core of radius r_0 is at a height H_0 above the surface of a flat solid screen (Fig. 1). Under the action of the self-induction, the ring vortex begins to move as a unit down to the screen. As the initial velocity field, the nonviscous solution for a ring vortex [2] is used. In the ideal-fluid approximation, the rate of self-induction V_0 of a ring solid vortex with a small-radius core of circular cross section, i.e., the velocity of travel of the center of mass of the vortex core along the symmetry axis, is estimated by the asymptotic formula [2]

$$V_0 = \Gamma_0 \frac{\ln (8R_0/r_0) - 0.25}{4\pi R_0}.$$

N. E. Zhukovskii Central Aerohydrodynamics Institute, 1 Zhukovskii Str., Zhukovskii, Moscow Obl., 140180, Russia; email: vlana@progtech.ru. Translated from Inzhenerno-Fizicheskii Zhurnal, Vol. 81, No. 1, pp. 184–190, January–February, 2008. Original article submitted April 13, 2007.

1062-0125/08/8101-0196©2008 Springer Science+Business Media, Inc.

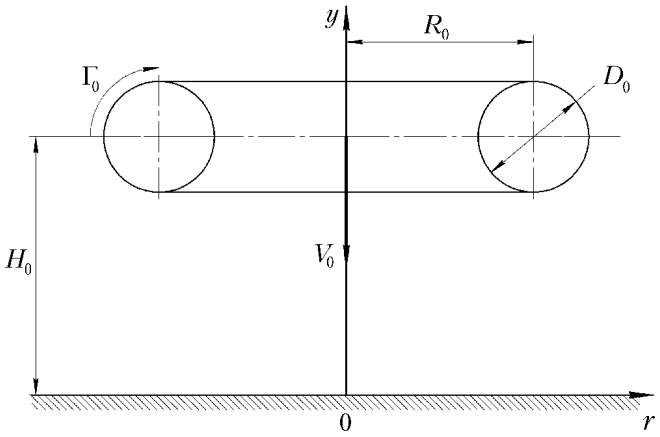

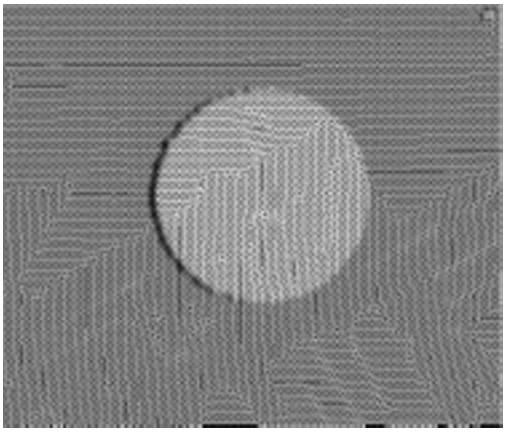

Fig. 1. Geometry of a ring vortex near a flat screen at the initial instant of time in the vertical diametrical plane of symmetry.

Fig. 2. Triangular grid in the first quadrant of the vertical symmetry plane of the problem.

The characteristic Reynolds number of the problem is determined by the rate of self-induction of the vortex and its diameter at the initial instant of time: $\mathrm{Re} = V_0 D_0/\nu$. The core of the vortex represents a constant-vorticity region, and the vortex circulation Γ_0 is determined as the product of the vorticity-vector module by the area of the circular cross section of the vortex core:

$$\Gamma_0 = |\boldsymbol{\omega}| \cdot 4\pi r_0^2 .$$

The velocity of the fluid in the core changes along its radius by the linear law; at the center of the core, it is equal to zero.

Thus, as the initial approximation (at the instant t_0) for numerical integration of the Navier–Stokes equations, the known solution obtained for an ideal (nonviscous) fluid is used.

The nonstationary Navier–Stokes equations defining the dynamics of the viscous interaction of a ring vortex with a near-wall turbulent flow on a flat screen are solved in a computational region representing an axisymmetric sector with an angular opening of 5°, in which a nonstructured hybrid tetrahedral-prismatical grid containing 0.5 mln nodes is generated. The algorithms and methods, used for construction and adaptation of irregular grids, as applied to the two- and three-dimensional problems of mathematical physics and computational gas dynamics, are original developments of the author and are described in [11–14]. For representation of the turbulent axisymmetric near-wall flow induced on the surface of the flat screen by the ring vortex moving to the screen with a required resolution, 15 grid layers consisting of prismatic cells pressed against the surface of the screen and extended strongly along it were generated crosswise to the thin near-wall layer. To adequately describe the evolution of the primary ring vortex moving to the screen in the process of its viscous interaction with the near-wall layer on the screen, as well as the formation of the secondary ring vortices with circulations opposite in sign as a result of the separation at different instants of time of the turbulent near-wall layer on the screen and their development, we generated a fairly fine grid, such that many grid cells were in the core of a vortex (in the grid shown in Fig. 2, 60 triangular cells are positioned along the diameter of the core).

Results of Calculations. The calculations were carried out with the ANSYS/CFX program complex on a two-core personal computer with a Pentium-D processor, operating at 3.2 GHz, and an on-line storage of 4 GB, which was controlled by a Linax SuSE10.0 ×86_64 operational system. The nonstationary Navier–Stokes equations were numerically integrated in the computational region representing an axisymmeric sector with an angular opening of 5°, a height of $1.5H_0$, and a length of $2.5H_0$ (in the radical direction in the cylindrical coordinate system), in which a nonstructured hybrid tetrahedral-prismatic grid containing 0.5 mln nodes was generated, and a triangular grid containing

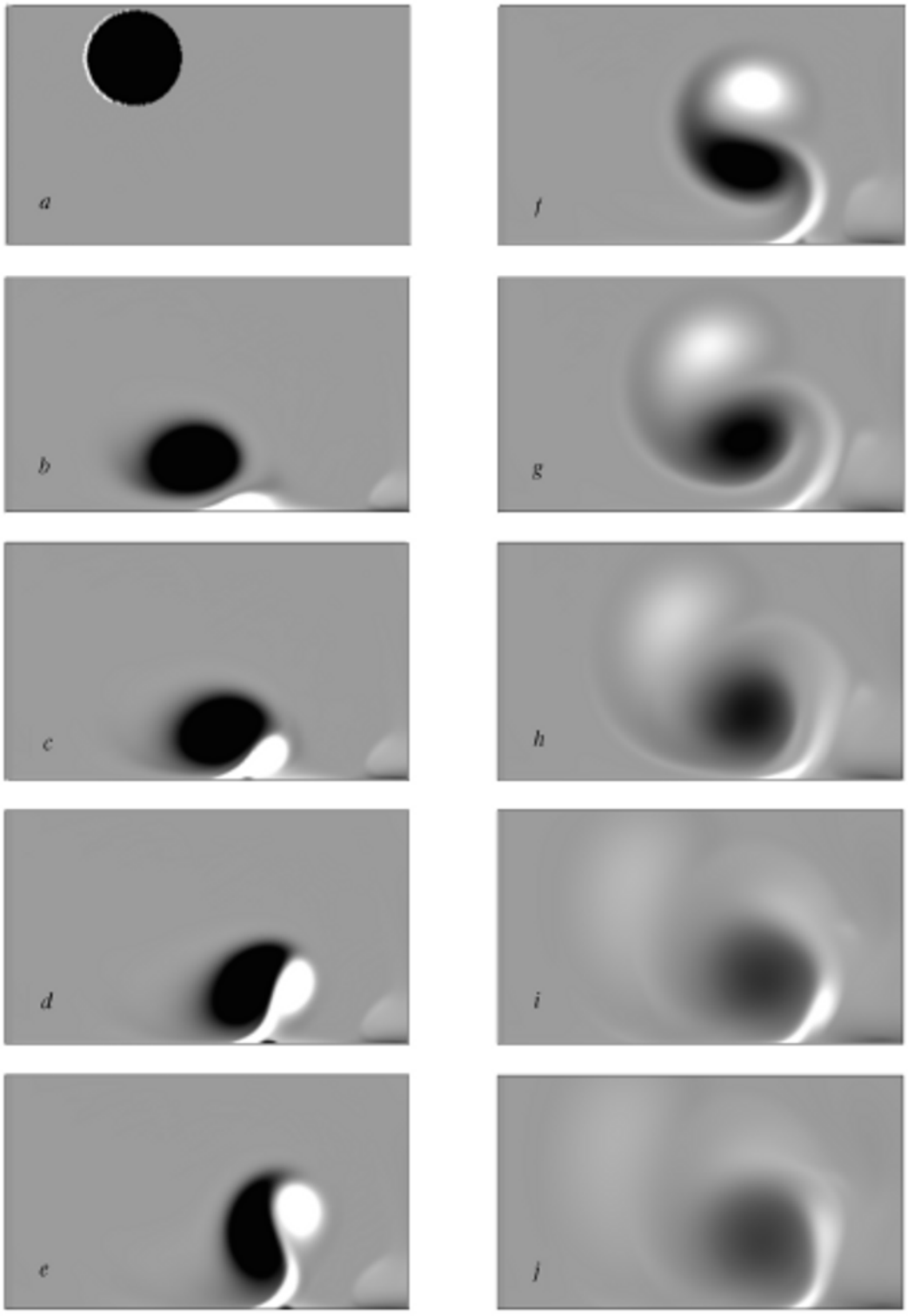

Fig. 3. Distribution of the vorticity ω (the grey-colored gradations, from the white to the black color correspond to the values of ω changing from –0.1 sec^{-1} to 0.15 sec^{-1} respectively) in the axial symmetry plane at Re = 10^5, r_0 = 2.5 m, H_0 = 10 m, R_0 = 10 m (the size of each fragment along the horizontal is 25 m) at different instants of time: t = 0 (a), 140 (b), 160 (c), 180 (d), 200 (e), 240 (f), 280 (g), 320 (h), 400 (i), and 440 sec (j).

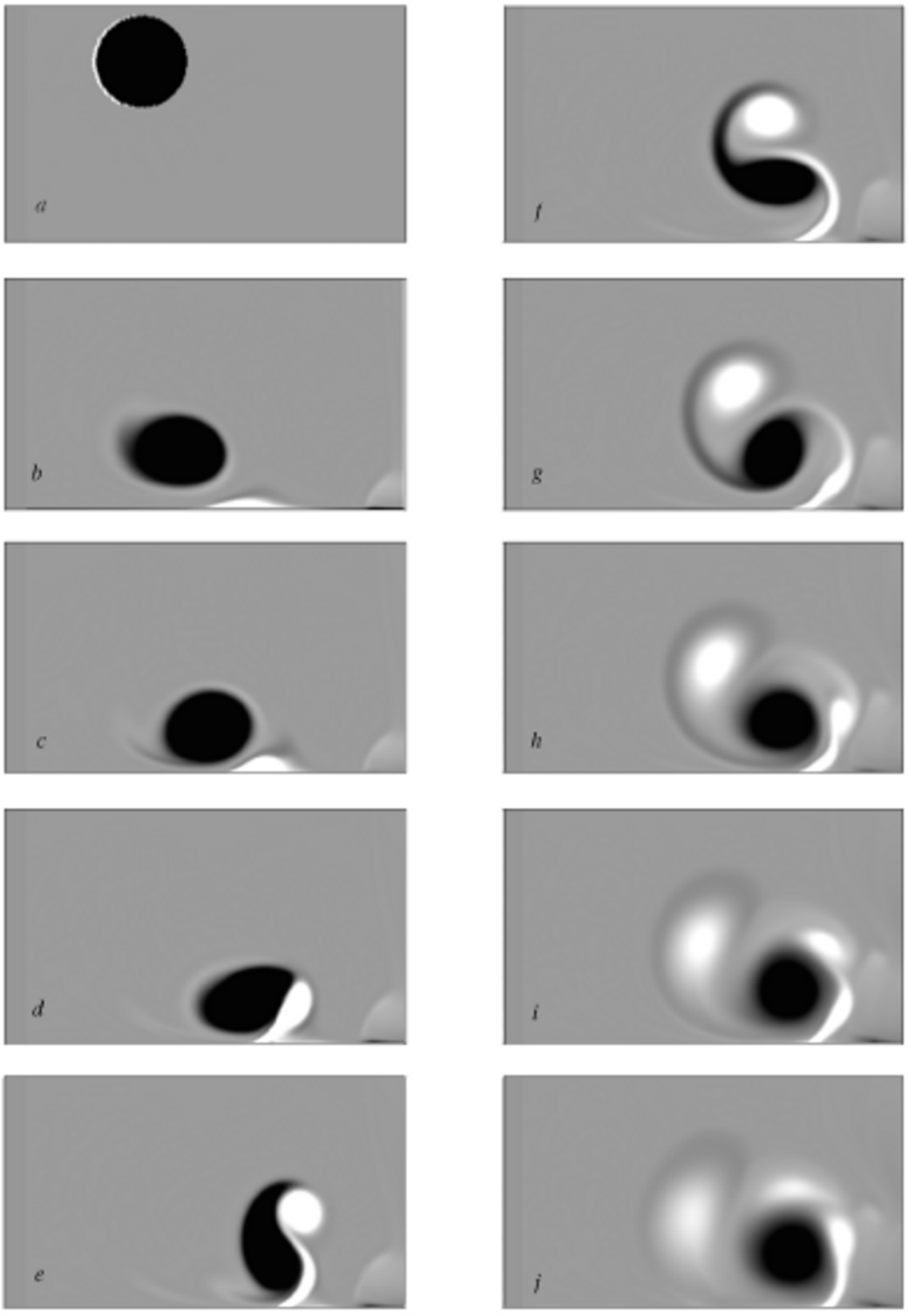

Fig. 4. Distribution of the vorticity ω (the grey-colored gradations, from the white to the black color correspond to the values of ω changing from −10.0 sec^{-1} to 15.0 sec^{-1} respectively) in the axial symmetry plane at Re = 10^7, r_0 = 2.5 m, H_0 = 10 m, R_0 = 10 m (the size of each fragment along the horizontal is 25 m) at different instants of time: t = 0 (a), 1.25 (b), 1.50 (c), 1.75 (d), 2.00 (e), 2.25 (f), 2.50 (g), 2.75 (h), 3.00 (i), and 3.25 sec (j).

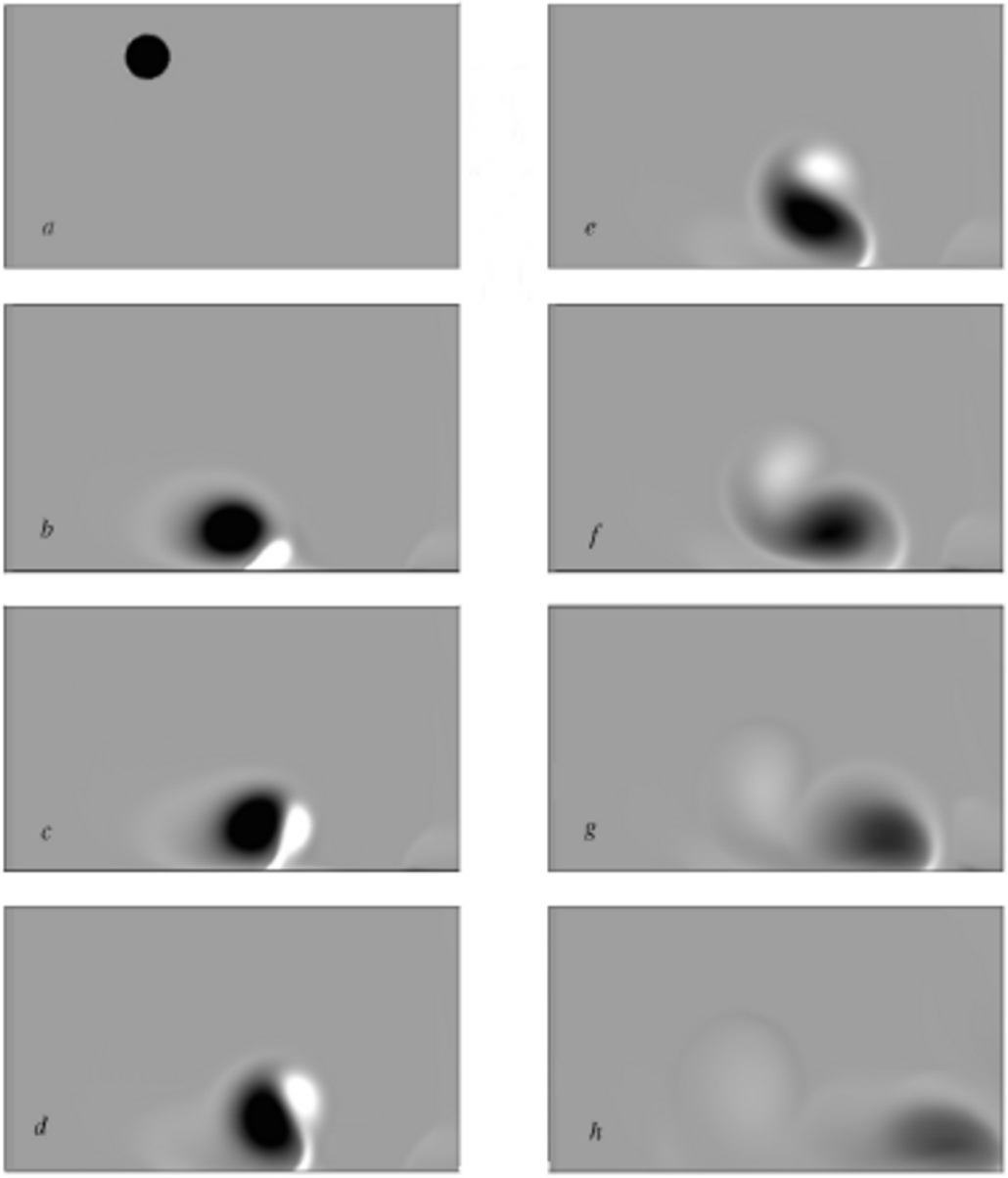

Fig. 5. Distribution of the vorticity ω (the grey-colored gradations, from the white to the black color, correspond to the values of ω changing from −25.0 sec^{-1} to 40.0 sec^{-1} respectively) in the axial symmetry plane at Re = 10^7, r_0 = 1.0 m, H_0 = 10 m, R_0 = 10 m (the size of each fragment along the horizontal is 25 m) at different instants of time: t = 0 (a), 1.1 (b), 1.3 (c), 1.4 (d), 1.5 (e), 1.7 (f), 2.0 (g), and 2.5 (h).

46,500 nodes was generated in the axial-symmetry plane. The calculations were performed for a ring vortex with the following geometric parameters: R_0 = 10 m, H_0 = 10 m, $r_0 = 0.1R_0$ and $0.25R_0$. The Reynolds numbers were changed within the range Re = 10^5–10^7. The step of integration of the equations of motion with respect to time was selected on the basis of a numerical experiment; its dimensionless value, determined from the expression $\Delta t_1 = \Delta t\Gamma_0/R_0^2$, was equal to 0.022, which corresponds to the dimensional time steps Δt = 1.0 sec for the flow at Re = 10^5 and Δt = 0.01 sec for the flow at Re = 10^7. The time of evolution of the ring vortex, determined numerically, comprised t_1 = 11 in the dimensionless form or, in the dimensional form, t = 500 sec at Re = 10^5 and t = 5 sec at Re = 10^7; for this time, the primary ring vortex reached the boundary of the computational region and was dissipated. A calculation of one

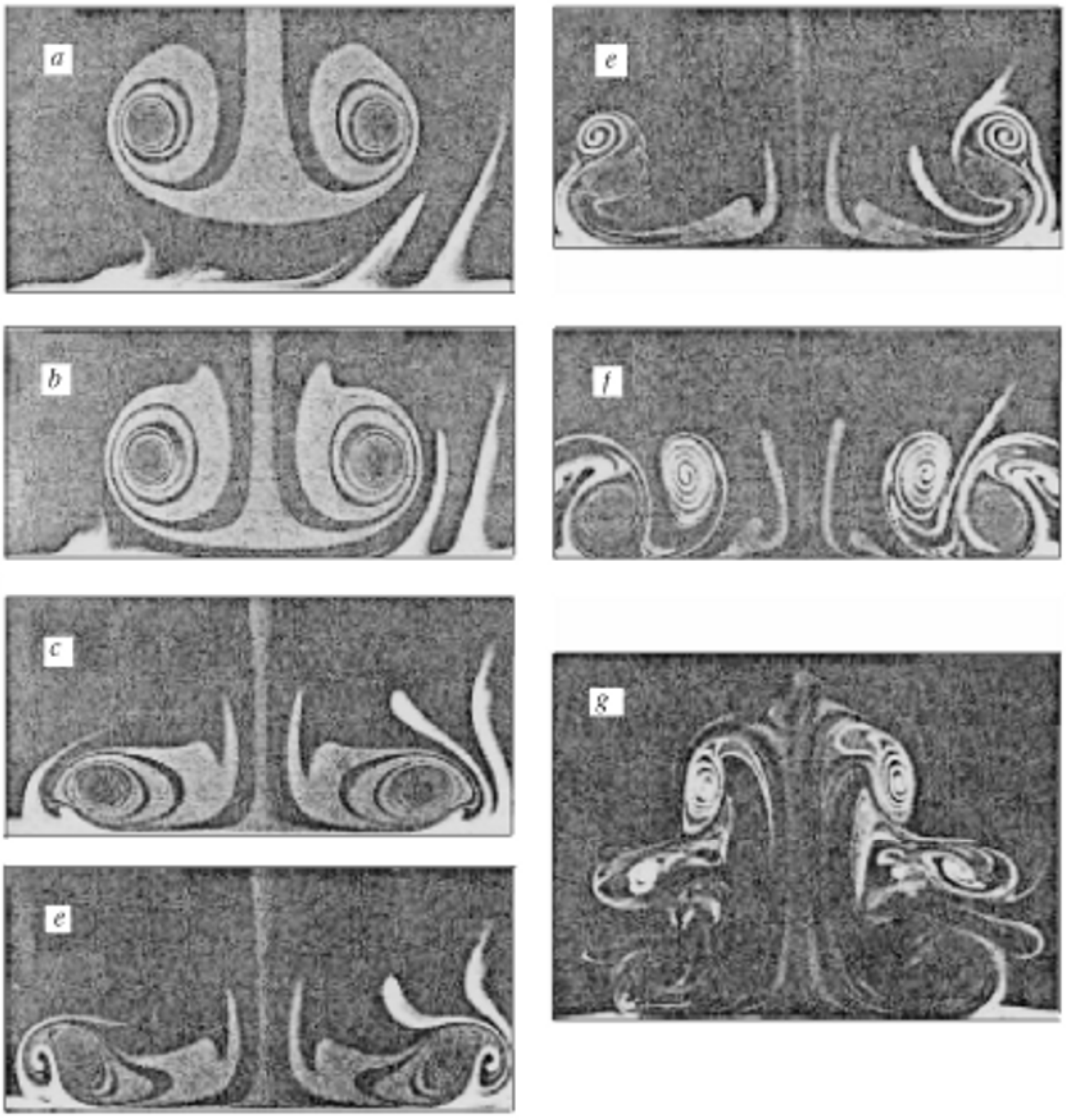

Fig. 6. Results of experimental investigations of the movement of a ring vortex near a flat screen under the laminar-flow conditions (Re = 930, the size of each fragment along the horizontal is 0.088 m) at different instants of time: t = 1.20 (a), 1.40 (b), 1.70 (c), 1.80 (d), 2.00 (e), 2.67 (f), and 3.80 (g).

variant of evolution of a ring vortex and the dynamics of its interaction with the turbulent neat-wall flow on the solid screen with the use of a two-core personal computer took 10–12 h.

In Figs. 3–5, patterns of the viscous interaction of a ring vortex with the turbulent near-wall layer on the screen, obtained for different instants of time, and patterns of formation and interference of the secondary ring vortices with the primary vortex in the form of vorticity fields, calculated for the characteristic Reynolds numbers Re = 10^5 and 10^7 and two values of the initial radius of the vortex core $r_0 = 0.25R_0$ and $0.1R_0$, are presented in the first quadrant of the vertical symmetry plane of the problem. The vorticity vector at each computational point was calculated by the formula $\omega = \mathrm{rot}\ \mathbf{V}$. The grey background in the figures corresponds to the zone of flow without separation, the black-colored regions correspond to the primary ring vortex, and the local white-colored regions correspond to the secondary ring vortices with vorticities opposite in sign.

These patterns clearly represent the dynamics of interaction of the primary ring vortex with the flat solid screen in the process of its movement to the screen and propagation along the screen plane in the direction from the

symmetry axis. As the vortex approaches the screen, its circular core (black-colored circle) initially changes its shape and arranges itself into an ellipse with the major axis directed parallel to the screen (the core of the vortex is extended along the screen). At the same time, the ring vortex moving to the screen stimulates the formulation of a nonstationary flow on the screen surface due to the formation of a turbulent axisymmetric near-wall layer. This near-wall layer grows ("swells") in the initial period of its formation; then the negative pressure gradient arising along the radius of the core changes to positive and there arise preseparation conditions where the region of the "swollen" boundary layer is extended in the vertical direction and forms a topology in the form of a drop "on a knife." Finally, the near-wall layer separates with formation of a series of secondary ring vortices with vorticities opposite in sign (local white-colored zones in the figures). Initially the secondary vortex is "coiled" on the core of the primary vortex that continues to move slowly along the screen in the direction from the symmetry axis; then this vortex separates, moves up to the symmetry axis, and, in doing so, runs ahead of the core of the primary vortex. It is clearly seen from Fig. 4 that several secondary vortices are generated at successive instants of time and a configuration of three secondary ring vortices is formed. In this case, the whole system of primary and secondary ring vortices slows down its motion along the screen and moves slowly up. With time, a viscous diffusion of the primary and secondary ring vortices is realized, the vortex system dissociates gradually, and the flow decays.

Conclusions. The results of our numerical calculations of the nonstationary viscous interaction of primary and secondary ring vortices near a flat screen and the flow patterns obtained agree qualitatively with the data obtained in [1] with the use of the discrete-vortex method and the boundary-layer theory as well as with the results of laboratory experimental investigations of the interaction of a ring vortex with a screen, obtained for laminar-flow conditions at small Reynolds numbers (see, e.g., Fig. 6 taken from [4]).

The author expresses her thanks to A. S. Ginevskii for interest in the numerical investigation of the problem considered, scientific support, and discussion of the results obtained.

NOTATION

D_0, diameter of a ring vortex at the initial instant of time, m; H_0, height of the vortex ring above a flat screen at the initial instant of time, m; r, coordinate axis of the cylindrical coordinate system directed along the radius of the vortex core; r_0, radius of the core of the ring solid vortex at the initial instant of time, m; R_0, radius of the ring vortex at the initial instant of time, m; $\mathrm{Re} = V_0 D_0/\nu$, characteristic Reynolds number; t, time, sec; t_1, dimensionless time; t_0, initial instant of time, sec; Δt, step of integration with respect to time, sec; Δt_1, dimensionless step of integration with respect to time; V_0, self-induced velocity of travel of the center of mass of the ring solid vortex along the vertical symmetry axis at the initial instant of time, m/sec; $\mathbf{V}$, velocity vector of a flow, m/sec; y, coordinate axis of the cylindrical coordinate system directed vertically up; Γ_0, circulation of the ring vortex, m^2/sec; ν, kinematic viscosity coefficient of air, m^2/sec; ω, vorticity vector, sec^{-1}.

REFERENCES

1. A. S. Ginevskii, T. V. Pogrebnaya, and S. D. Shipilov, Propagation of a ring vortex over a flat screen, *Fiz. Atmos. Okeana*, **42**, No. 5, 1–5 (2006).
2. O. G. Goman, V. I. Karplyuk, M. I. Nisht, and A. G. Sudakov (M. I. Nisht Ed.), *Numerical Simulation of Axisymmetric Separation Incompressible Liquid Flows* [in Russian], Mashinostroenie, Moscow (2000).
3. F. J. Saffman, *Dynamics of Vortices* [Russian translation], Nauchnyi Mir, Moscow (2000).
4. A. M. Naguib and M. M. Koochessfahani, On wall-pressure sources associated with the unsteady separation in a vortex-ring wall interaction, *Phys. Fluids*, **16**, No. 7, 2613–2622 (2004).
5. J. D. A. Walker, C. R. Smith, A. W. Cerra, and T. L. Doligalski, The impact of a vortex ring on a wall, *J. Fluid Mech.*, **181**, 99–140 (1987).
6. C. P. Gendrich, D. G. Bohl, and M. M. Koochesfahani, Whole-field measurements of unsteady separation in a vortex ring wall interaction, *AIAA Paper*, No. 97—1780 (1997).
7. D. Fabris, D. Liepmann, and D. Marcus, Quantitative experimental and numerical investigation of a vortex ring impinging on a wall, *Phys. Fluids*, **8**, 2640 (1996).

8. C. C. Chu, C. T. Wang, and C. C. Chang, A vortex ring impinging on a solid plane surface: Vortex structure and surface force, *Phys. Fluids*, **7**, 1391 (1995).
9. Fluid vortices, in: Sheldon I. Green (Ed.), *Fluid Mechanics and Its Applications*, Vol. 30, ISBN 0-7923-3376-4, Kluwer Academic Publishers, Netherlands (1995).
10. F. R. Menter, Two-equation eddy-viscosity turbulence models for engineering applications, *AIAA J.*, **32**, No. 8, 1598–1605 (1994).
11. N. A. Vladimirova and A. M. Sorokin, Anisotropic adaptation of three-dimensional irregular grids in the problems of computational gas dynamics, *Zh. Vych. Mat. Mat. Fiz.*, **43**, No. 6, 909–919 (2003).
12. N. A. Vladimirova and A. M. Sorokin, Anisotropic adaptation of three-dimensional irregular grids in problems of computational fluid dynamics, *Comput. Math. Math. Phys.*, **43**, No. 6, 870–879 (2003).
13. N. A. Vladimirova and A. M. Sorokin, Use of anisotropic adaptation for numerical solution of two- and three-dimensional problems of gas dynamics on nonstructured grids, *Aéromekh. Gaz. Din.*, No. 3, 21–30 (2003).
14. A. M. Sorokin and N. A. Vladimirova, Anisotropic grid adaptation applied to aerodynamic problems, in: O. V. Ushakova (Ed.), *Advances in Grid Generation*, ISBN 1-59454-273-2, Nova Science Publishers Inc., New York, USA (2007), pp. 189–212.